



Diode-pumped 1- μm Nd:YVO₄ and Nd:YLF lasers with active thermal lensing compensation and manipulated beam quality

SHOU-TAI LIN* AND CHENG-PO CHEN

Department of Photonics, Feng Chia University, No.100 Wenhwa Road, Seatwen, Taichung 407802, Taiwan
*stailin@mail.fcu.edu.tw

Abstract: Thermally induced optical adaptive lens in a solid-state laser can be used to compensate for the thermal lens and improve the beam quality. Herein, we present an active compensation method for thermal lensing in 1 μm diode-pumped solid-state Nd:YVO₄ and Nd:YLF lasers. The compensation scheme comprised thermally inducing the defocusing effect of π polarization in Nd:YLF; the defocusing strength was controlled using a diode pump power. By varying the absorbed ~ 790 nm diode power of Nd:YLF (0 to 7.8 W), the beam quality, M^2 , of Nd:YVO₄ was manipulated from 2.4 to ~ 1.1 and the power fluctuation was measured to be less than 0.5%.

© 2022 Optica Publishing Group under the terms of the [Optica Open Access Publishing Agreement](#)

1. Introduction

Diode-pumped solid-state (DPSS) laser systems have been widely used in material processing, scientific research, and medical applications owing to their advantages of compactness, reliability, and high efficiency. In an end-pumping scheme, high quality output beam can be achieved through the design of spatial mode matching between the pump mode and fundamental cavity mode. The scaling of end-pumped lasers to high powers and nonuniform heating within the laser medium induces thermal distortion, including birefringence and lensing effects [1]. Thermally induced birefringence can cause significant power loss. Intracavity quarter-waveplates [2], optimized laser crystal cuts [3], and slab laser schemes [4] have been proposed to eliminate birefringence. Moreover, the thermally induced lens creates unstable beam parameters and poor beam quality. Various passive and active schemes have been proposed to compensate for the thermally induced lens effect. Passive compensation methods generally use a concave lens or a refractive index material with a negative temperature coefficient (dn/dT), for example, Poly (methyl methacrylate) (PMMA) [5], to cancel the thermal lens effect of the laser medium. However, the concave lens can only compensate certain pump power level and the thermally induced defocusing lens in Poly is varied with the pumping power. Therefore, the passive techniques narrowed the output power range and limited the beam quality. Active schemes, involving intracavity deformable mirrors based on micromachined membranes [6] and pneumatic actuation [7,8], have been successfully demonstrated to actively compensate for the thermal lensing effect with improved power scaling and beam quality. Modulating the curvature of the deformable mirror, the temporal control of the radiation parameters can also be reached. Another active scheme, side-pumped dual rod Nd:YLF laser, has also showed the increased stability and superior beam quality [9]. However, there is no study of dual rod thermal compensation in end-pumped scheme. In this paper, an end-pumped laser-controlled for actively compensating thermally induced lensing effect of the Nd:YVO₄ and Nd:YLF lasers with manipulated beam quality is reported, where Nd:YLF is pumped in π polarization with negative dn/dT for dynamically compensating for the positive thermal effect of Nd:YVO₄.

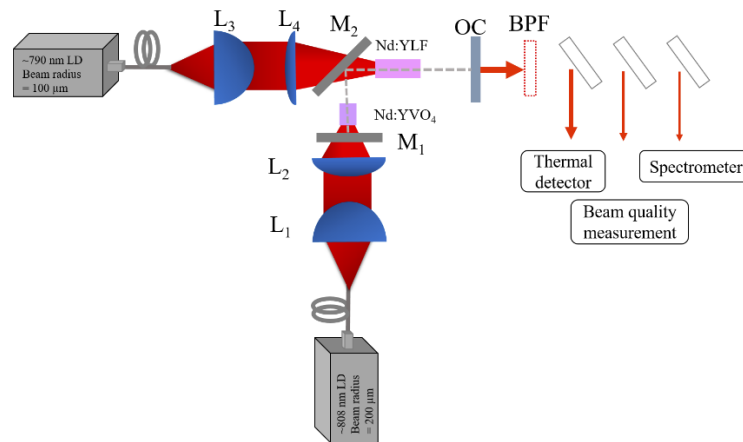


Fig. 1. Experimental setup of a thermal compensation Nd:YVO₄/Nd:YLF laser.

2. Experimental setup

A schematic of the thermal compensation Nd:YVO₄/Nd:YLF laser is shown in Fig. 1. The laser comprised an L-shaped cavity with two a-cut, $3 \times 3 \text{ mm}^2$ aperture, gain mediums: 5 mm long, 0.5 at.% doped Nd:YVO₄ crystals and 20 mm long, 1 at.% doped Nd:YLF crystals. To dissipate the heat generation, the crystals were wrapped by indium foil and kept in a copper block for water cooling at 25 °C. Two fiber coupled diode lasers, wavelengths with ~808 and ~790 nm, were used to separately pump the Nd:YVO₄ and Nd:YLF crystals. Coupling lenses L₁, L₂, L₃, and L₄ were used to refocus the beam radius of two pump beams to ~550 μm in the gain mediums. The ~790 nm diode laser was adopted because the absorption coefficient of π polarization in Nd:YLF has two times larger than σ polarization at this wavelength [10]. Moreover, π polarization of Nd:YLF exhibits a negative thermal-optics coefficient ($dn/dT = -4.3 \times 10^{-6}$) [11] and thermal defocusing behavior. Although the σ polarization of Nd:YLF exhibits a negative thermal-optics coefficient ($dn/dT = -2.0 \times 10^{-6}$), a slightly positive thermal lensing is observed after considering the bulge effect of the end faces [11]. To purify the study of π polarization and thermal defocusing behavior in Nd:YLF, an L-shaped cavity design was adopted to prevent the excitation of σ polarization by the ~808 nm diode laser. To process the thermal compensation scheme, the π polarization of both laser gain media was aligned in parallel. When the π polarization of the two laser gain media was aligned in the orthogonal direction, the thermal compensation scheme was not observed. The cavity was constructed using three flat mirrors: M₁, M₂, and OC. The distance between the two laser crystals was 2.5 cm and the total cavity physical length was maintained at approximately 11 cm. M₁ and M₂ possessed coatings with anti-reflection at ~800 nm and high reflectance (>99%) at 1040–1070 nm. The gain mediums possessed anti-reflection coatings at ~800 and 1040–1070 nm on both the interfaces. OC possessed a partial reflectivity ($R = 85\%$) in the range of 1040–1070 nm. To ensure that the thermally induced temperature distributions of the two gain mediums were spatially overlapped, the Nd:YVO₄ laser was constructed at the beginning, and the 790 nm diode laser was aligned by a 3-axis translation stage to match the 1064 nm spatial position in the Nd:YLF laser medium. A thermal detector and spectrometer (resolution: 1 nm) were used to monitor the average output power and wavelength, respectively. A band pass filter (BPF, Thorlabs FLH1064-10), with a center wavelength of 1064 nm and bandwidth of 10 nm, was used to block the 1047 nm wavelength and measure the output performance at 1064 nm. The transmittance of BPF at 1064 nm was first characterized by only turning on an ~808 nm diode laser. An output power of 1047 nm can be deduced by comparing

the total output power with and without BPF. A beam profiler (DataRay, WinCamD M2DU) equipped with a linear motorized stage and a 44 mm traveling range was constructed to monitor the far-field spatial mode and characterize the beam quality.

3. Results and discussions

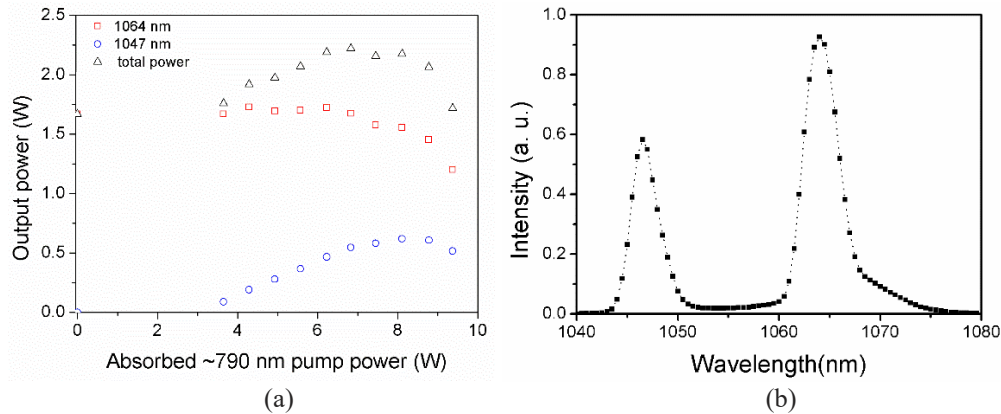


Fig. 2. (a) Measured output power of 1064 and 1047 nm versus absorbed ~790 nm diode power, (b) Measured outputs spectrum of 1064 and 1047 nm when the absorbed ~808 and ~790 nm diode power were 10.6 and 8 W, respectively.

Figure 2(a) shows the measured Nd:YVO₄/Nd:YLF laser output power when the absorbed ~808 and ~790 nm diode powers were maintained at ~10.6 W and varied between 0 and 10 W, respectively. When the absorbed ~790 nm diode power was higher than 4 W, we observed the generation of 1047 nm laser using a real-time spectrometer, as shown in Fig. 2(b). The output power of 1047 nm increased monotonically when the absorbed ~790 nm diode power was lower than 8 W. Once the absorbed diode power was higher than 8 W, the cavity was run into the unstable regime, and the thermal crack issue [11] of Nd:YLF occurred occasionally. Furthermore, the σ polarization of Nd:YLF (1053 nm) and gain competition between 1047 and 1053 nm were appeared [12]. To prevent thermal cracking, the absorbed ~790 nm diode power was maintained below 8 W in the following measurement. Before analyzing the thermal compensation in detail, we first estimated the focal length of the thermal lens in Nd:YVO₄. When the ~790 nm diode power was turned off, the 1064 nm output power corresponding to different cavity lengths was recorded, where the OC position was varied [13], as shown in Fig. 3. The focal length of the thermal lens of Nd:YVO₄ was measured to be shorter than 400 mm, and the beam radius of TEM₀₀ inside Nd:YVO₄ was calculated to be smaller than 280 μ m using the ABCD matrix method [14]. Although the current method cannot accurately measure the focal length of the thermal lens, it can provide a rough estimation. A more accurate experimental determination of the thermal lens in the laser crystals can be reached by intra-cavity adaptive optics [15]. Because the radius ratio between the pumping and cavity modes reached ~2, the current cavity design was favorable for producing a high-order transverse mode. In the following measurements, we set the absorbed ~808 nm diode power at 10.6 W. Figure 4 shows the measured beam profiles of 1064 nm at varied absorbed ~790 nm diode power. Once the ~790 nm diode power was increased, the mismatched mode matching of 1064 nm was compensated by the thermally induced defocusing lens of Nd:YLF. Therefore, the beam profile of 1064 nm was transferred into the fundamental mode when the absorbed ~790 nm diode power reached 7.5 W, as shown in Fig. 4(h). The response time to reach the stable beam profile was less than 1 s, which was limited by the response time of the beam profiler. A slight spatial alignment of the ~790 nm

diode laser was required to ensure coaxial propagation between 1047 and 1064 nm. Without symmetric thermal compensation, an elliptical beam shape was observed, as shown in Fig. 4(j). In the following measurements, the cavity was maintained in a coaxial alignment between two wavelengths without notification. We also recorded a beam profile of 1047 nm at the same power level of Fig. 4(i), as shown in Fig. 4(k), and only the fundamental mode was observed in the operated power range. From these results, the following two conclusions were derived. First, the thermal defocusing behavior of 1047 nm cannot be stable in the flat/flat cavity, without the help of positive thermal lensing, contributed by 1064 nm. Second, the small signal gain of 1047 nm must be larger than the cavity loss. When the diode power of ~ 790 nm was increased and the cavity threshold was overcome, the fundamental mode of 1047 nm was excited first. While the thermally induced defocusing lens was incorporated into the cavity, the fundamental cavity mode of 1064 nm was dynamically expanded by the compensation scheme, and the fundamental mode of 1047 nm was expanded in the same way. Therefore, only the fundamental mode at 1047 nm was observed during the measurements.

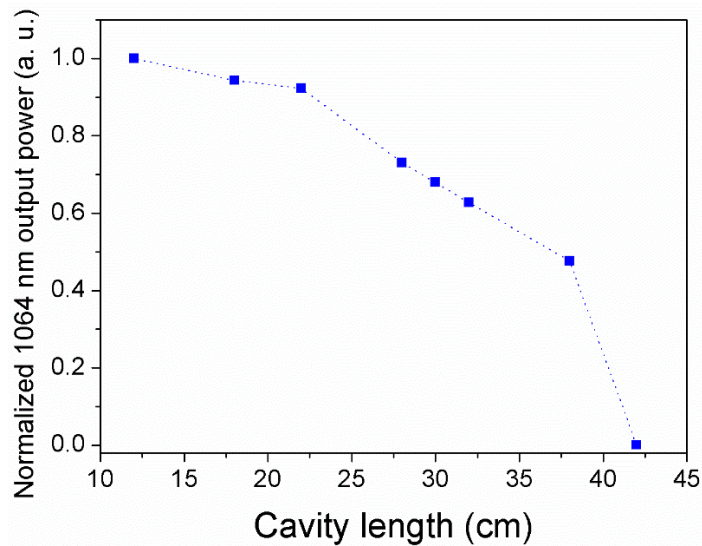


Fig. 3. Measured output power of 1064 nm by varying the cavity length when the ~ 790 nm diode laser was turned off.

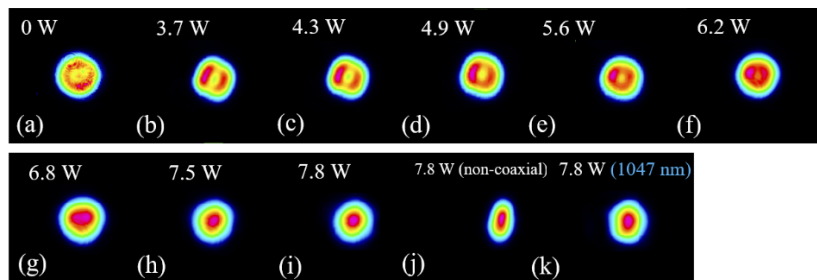
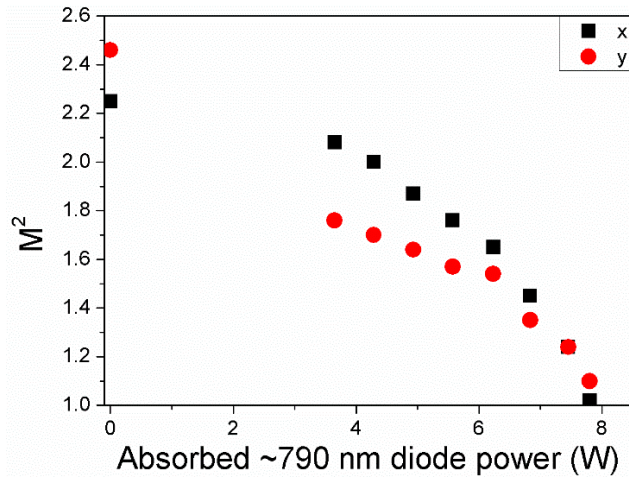
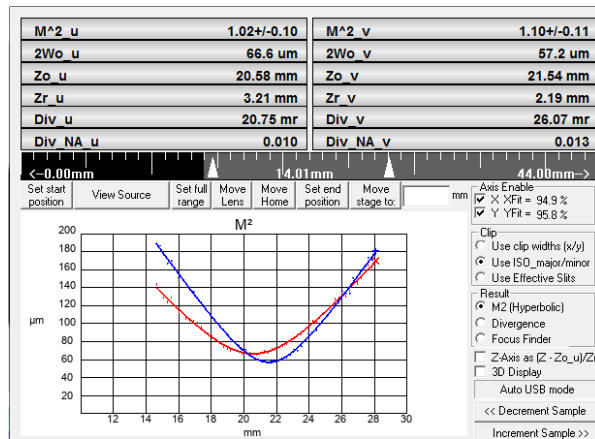


Fig. 4. Recorded far-field patterns of 1064 nm under thermal compensation for the absorbed ~ 808 nm diode power was fixed at 10.6 W. The absorbed ~ 790 nm diode power was shown in the inset. The elliptical beam profile of 1064 nm under non-coaxial propagation and typical 1047 nm pattern were recorded as a comparison.



(a)



(b)

Fig. 5. (a) Measured beam quality, M^2 , of 1064 nm vs. absorbed ~790 nm diode power. (b) M^2 fitting result at absorbed ~790 nm diode power of 7.8 W, where u and v are represented as x and y, respectively.

To characterize the beam quality of 1064 nm laser, a 100 mm focal lens was adopted to refocus the beam profiler, and the M^2 value was fitted using the ISO-11146 method, as shown in Fig. 5(a). Without thermal compensation (~ 790 nm diode laser was turned off), the M^2 of the x and y directions were measured to be 2.25 and 2.45, respectively. The discrepancy of the M^2 -values between the x- and y-directions was caused by the mounting concept of the laser crystal which resulted in a non-symmetric thermal distribution inside the laser gain medium. With thermal compensation (~ 790 nm diode laser was turned on), M^2 was reduced gradually and reached ~ 1.1 for both x and y directions when the absorbed ~ 790 nm diode power reached 7.8 W. The typical M^2 measurements and fitting results are shown in Fig. 5(b). Owing to the L-shaped cavity design and astigmatism effect, a slightly different waist position between the x and y directions was revealed. Comparing the results in Figs. 4 and 5, the M^2 measurements coincided with the observed beam profiles. This is the first report on laser beam quality that can be manipulated using optical power. To study the stability of thermal compensation, an output power of 1064 nm was recorded using a thermal detector. Figure 6 shows the 10 min power fluctuation versus the absorbed ~ 790 nm diode power. Although the power fluctuation in the scheme of thermal compensation was increased from 0.2% to 0.4%, the power stability was still acceptable for further applications.

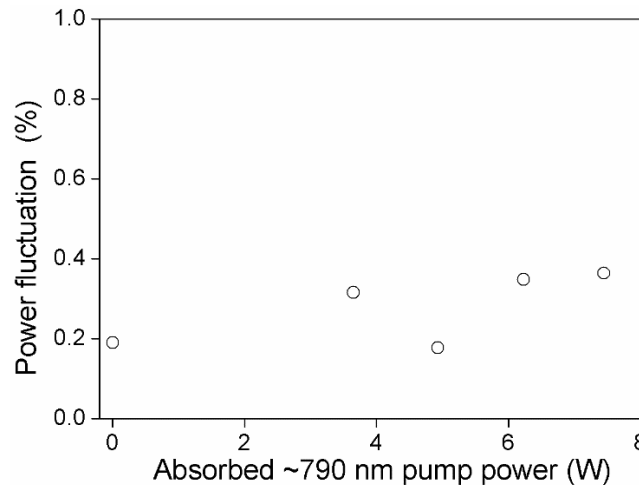


Fig. 6. Measured 10 min power stability of 1064 nm vs. absorbed ~ 790 nm diode power.

Conclusions

In conclusion, we demonstrated a Nd:YVO₄ and Nd:YLF laser with dynamic thermal lensing compensation in the 1- μ m range. By measuring the spatial modes and beam quality of Nd:YVO₄ laser at different absorbed ~ 790 nm diode power in Nd:YLF crystal, the thermally induced defocusing of π polarization in Nd:YLF can provide an active scheme to compensate for thermally induced focusing. The power fluctuation of Nd:YVO₄ laser was better than 0.5% under thermal lensing compensation. Although we only present the results in a cw, watt level laser scheme, the preliminary data of pulsed laser scheme, inserting AO Q-switch element into Fig. 1, also reveal the similar compensation behavior. The achievement in this report can be regarded as an oscillator and amplified by master oscillator power amplifier approach (MOPA) [16] for high power application. Another future scope will be the spatial beam manipulation of Nd:YVO₄ laser through varying the beam shape of ~ 790 nm diode laser or spatial overlapping between two pump lasers.

Funding. Ministry of Science and Technology, Taiwan (110-2221-E-035 -056 -MY2, MOST 108-2119-M-030 -001-MY2, MOST 109-2221-E-035-072).

Disclosures. The authors declare no conflicts of interest.

Data availability. Data underlying the results presented in this paper are not publicly available at this time but may be obtained from the authors upon reasonable request.

References

1. W. A. Clarkson, "Thermal effects and their mitigation in end-pumped solid-state lasers," *J. Phys. D: Appl. Phys.* **34**(16), 2381–2395 (2001).
2. W. A. Clarkson, N. S. Felgate, and D. C. Hanna, "Simple method for reducing the depolarization loss resulting from thermally induced birefringence in solid-state lasers," *Opt. Lett.* **24**(12), 820–822 (1999).
3. O. Puncken, H. Tünnermann, J. J. Morehead, P. Weßels, M. Frede, J. Neumann, and D. Kracht, "Intrinsic reduction of the depolarization in Nd:YAG crystals," *Opt. Express* **18**(19), 20461–20474 (2010).
4. J. S. Shin, Y.-H. Cha, G. Lim, Y. Kim, S. O. Kwon, B. H. Cha, H. C. Lee, S. Kim, K. U. Koh, and H. T. Kim, "Wavefront improvement in an end-pumped high-power Nd:YAG zigzag slab laser," *Opt. Express* **25**(16), 19309–19319 (2017).
5. H. Yoshida, N. Takeuchi, H. Okada, H. Fujita, and M. Nakatsuka, "Thermal-lens-effect compensation of Nd:YAG rod laser using a solid element of negative temperature coefficient of refractive index," *Jpn. J. Appl. Phys.* **46**(3A), 1012–1015 (2007).
6. G. Vdovin and V. Kiyko, "Intracavity control of a 200-W continuous-wave Nd:YAG laser by a micromachined deformable mirror," *Opt. Lett.* **26**(11), 798–800 (2001).
7. S. Piehler, B. Weichelt, A. Voss, M. A. Ahmed, and T. Graf, "Power scaling of fundamental-mode thin-disk lasers using intracavity deformable mirrors," *Opt. Lett.* **37**(24), 5033–5035 (2012).
8. S. Piehler, T. Dietrich, P. Wittmüss, O. Sawodny, M. A. Ahmed, and T. Graf, "Deformable mirrors for intra-cavity use in high-power thin-disk lasers," *Opt. Express* **25**(4), 4254–4267 (2017).
9. H. Vanherzeele, "Continuous wave dual rod Nd:YLF laser with dynamic lensing compensation," *Appl. Opt.* **28**(19), 4042–4044 (1989).
10. J. R. Ryan and R. Beach, "Optical absorption and stimulated emission of neodymium in yttrium lithium fluoride," *J. Opt. Soc. Am. B* **9**(10), 1883–1887 (1992).
11. P. J. Hardman, W. A. Clarkson, G. J. Friel, M. Pollnau, and D. C. Hanna, "Energy-transfer upconversion and thermal lensing in high-power end-pumped Nd:YLF laser crystals," *IEEE J. Quantum Electron.* **35**(4), 647–655 (1999).
12. H. C. Liang and C. S. Wu, "Diode-pumped orthogonally polarized self-mode-locked Nd:YLF lasers subject to gain competition and thermal lensing effect," *Opt. Express* **25**(12), 13697–13704 (2017).
13. F. Song, C. Zhang, X. Ding, J. Xu, G. Zhang, M. Leigh, and N. Peyghambarian, "Determination of thermal focal length and pumping radius in gain medium in laser-diode-pumped Nd:YVO₄ lasers," *Appl. Phys. Lett.* **81**(12), 2145–2147 (2002).
14. B. E. A. Saleh and M. C. Teich, *Fundamental of Photonics* (John Wiley & Sons, 2007), pp. 74–100.
15. W. Lubeigt, M. Griffith, L. Laycock, and D. Burns, "Reduction of the time-to-full-brightness in solid-state lasers using intra-cavity adaptive optics," *Opt. Express* **17**(14), 12057–12069 (2009).
16. M. Ostermeyer, P. Kappe, R. Menzel, and V. Wulfmeyer, "Diode-pumped Nd:YAG master oscillator power amplifier with high pulse energy, excellent beam quality, and frequency-stabilized master oscillator as a basis for a next-generation lidar system," *Appl. Opt.* **44**(4), 582–590 (2005).